Available online at www.sciencedirect.com
SCIENCE DIRECT®
Journal of Nuclear Materials 335 (2004) 501–507
journal of nuclear materials
www.elsevier.com/locate/jnucmat

Corrosion behavior of Al-surface-treated steels in liquid Pb–Bi in a pot

Y. Kurata *, M. Futakawa, S. Saito

Center for High Intensity Proton Accelerator Facilities, Tokai Research Establishment, Japan Atomic Energy Research Institute, Tokai-mura, Ibaraki-ken 319-1195, Japan

Received 2 September 2002; accepted 18 August 2004

Abstract

Corrosion tests were performed in oxygen-saturated liquid Pb–Bi at 450 °C and 550 °C in a pot for 3000 h for Al-surface-treated steels containing various levels of Cr contents. The Al surface treatments were achieved using a gas diffusion method and a melt dipping method. Al_2O_3, $FeAl_2$ and $AlCr_2$ produced by the gas diffusion method exhibited corrosion resistance to liquid Pb–Bi, while the surface layer produced by the melt dipping method suffered a severe corrosion attack. Fe_4Al_{13} and Fe_2Al_5 produced by the melt dipping method disappeared during the corrosion test at 550 °C and only FeAl remained.

PACS: 81.65.K; 28.41.T

1. Introduction

Liquid Pb–Bi has excellent properties as a spallation target and a coolant of an accelerator driven system (ADS) for the transmutation treatment of long-lived radioactive wastes [1,2]. However, corrosion of component materials is concerned since the solubility of Ni, Cr and Fe in liquid Pb–Bi is high [2,3]. Thus, the corrosion of the component materials in liquid Pb–Bi is one of the important research items in development program of the ADS [1,4]. In the long-term study in Russia, the following important points have been pointed out: corrosion behavior in liquid Pb–Bi depends on oxygen concentration in Pb–Bi and corrosion resistance is improved by formation of the protective oxide film which is achieved by introduction of oxygen controlling system in Pb alloy loops. For the operation of liquid Pb alloy loops, the control of oxygen potential is recommended to form Fe_3O_4 without PbO precipitation [2,5]. Recently, various corrosion tests in Pb alloys have been carried out actively to confirm the improvement effect and accelerate ADS development [6–12]. A liquid Pb alloy forced circulation loop where the liquid alloy flows through high and low temperature components, enables us to conduct corrosion tests under actual condition. On the other hand, corrosion tests in a pot are useful for screening various materials and for obtaining basic data on corrosion.

Corrosion/erosion properties in liquid Pb–Bi depend on many parameters such as testing temperature,

* Corresponding author. Tel.: +81 29 282 5059; fax: +81 29 282 6489.
E-mail address: ykurata@popsvr.tokai.jaeri.go.jp (Y. Kurata).

0022-3115/$ - see front matter © 2004 Elsevier B.V. All rights reserved.
doi:10.1016/j.jnucmat.2004.08.004

Table 1
Chemical composition of tested alloys (wt%)

	C	Cr	Ni	Mo	Fe	V	W
F82H	0.095	7.72	<0.02	<0.01	Bal.	0.01	1.95
Mod.9Cr–1Mo steel	0.10	8.41	0.06	0.88	Bal.	0.047	<0.0005
JPCA	0.058	14.14	15.87	2.29	Bal.	0.003	0.01
410SS	0.067	12.21	0.12	0.02	Bal.	0.013	–
430SS	0.08	16.24	0.15	0.02	Bal.	0.024	–
2.25Cr–1Mo steel	0.10	2.18	0.02	0.92	Bal.	0.009	–

temperature gradient between high and low temperature parts, flow velocity, flow pattern, oxygen concentration in liquid Pb–Bi, alloying elements in steels, concentration of dissolved elements, etc. In the case of corrosion tests in a pot, we can choose the parameters of the testing temperature, the oxygen concentration in Pb–Bi, the alloying elements in steels and the concentration of dissolved elements. Since corrosion/erosion resistance deteriorates under high temperature and high velocity conditions, improvement of corrosion/erosion resistance has been attempted by adopting coating and surface treatment [10–14]. As a result, Al-surface-treated alloys showed the improvement of corrosion resistance in liquid Pb [10,11] and Pb–Li [13,14] under very low oxygen potential conditions. However, sufficient data on Al-surface-treated alloys have not been available in liquid Pb–Bi.

In the case of ADS application, it is probable that oxygen potential in liquid Pb–Bi is very low in the spallation target area where high-energy protons are irradiated. However, as the Gibbs energy of Al_2O_3 formation is very low, it is expected that the protective Al_2O_3 layer can be formed on the surface of Al-surface-treated alloys under the low oxygen potential. Not only the beam window of the spallation target but also fuel rods, a reactor vessel, Pb–Bi pumps, steam generators are important parts in the ADS. It is supposed that the oxygen potential has a wide distribution in the ADS. Al-surface-treated alloys have the possibility of corrosion resistance to liquid Pb–Bi under a wide range of the oxygen potential.

Recently, Mueller et al. [12] reported the results of corrosion experiments in flowing Pb–Bi with an oxygen concentration of 10^{-6} wt% for Al-alloyed specimens produced by Al-wrapped and Al-dipped procedures. Specimens alloyed by Al-foil wrapping showed good corrosion resistance in flowing liquid Pb–Bi up to 600 °C, while a severe attack and penetration of Pb and Bi occurred even at 420 °C in specimens alloyed by Al-hot dipping. According to these results, corrosion resistances of Al-surface-treated alloys vary drastically depending on surface treatment methods.

Therefore, it is necessary to examine the effect of different Al-surface treatment methods on the corrosion properties in liquid Pb–Bi. The purpose of the present study is to investigate the effects of two types of Al surface treatment on corrosion behavior in Pb–Bi melt in a pot.

2. Experimental apparatus and procedure

2.1. Specimens and Al surface treatment

Steels used in the experiment were F82H steel, Mod.9Cr–1Mo steel, 14Cr–16Ni–2Mo steel(JPCA), 410SS, 430SS and 2.25Cr–1Mo steel, the chemical compositions of which are shown in Table 1. Table 2 shows specimen signatures. The Al surface treatments were achieved by two different methods: (1) gas diffusion treatment was done using Al compound powders (FeAl + Al_2O_3) and Ar carrier gas, and heating at 1100 °C for 10 h, and (2) melt dipping was done by hot-dipping in Al-melt and heating at 703 °C for 2 min.

Fig. 1 shows typical optical micrographs of cross-sections of Al-surface-treated specimens. In BD, CD and ED, layers produced by the gas diffusion treatment were not uniform and Al_2O_3 with dark contrast was formed. It was found from the results of X-ray diffraction in Table 3 that the layers are composed of Al_2O_3, $FeAl_2$ and $AlCr_2$. The thickness of the layer was measured by using optical microscope and electron probe micro-analyzer (EPMA). The Al concentration profile obtained by EPMA was used to determine the layer thickness of BD and ED specimens because it was not clear in optical

Table 2
Specimen signatures

Alloy	Surface treated Al-diffusion	Surface treated Al-melt dipping
F82H	AD	AM
Mod.9Cr–1Mo steel	BD	BM
JPCA	CD	CM
410SS	DD	DM
430SS	ED	EM
2.25Cr–1Mo steel	FD	FM

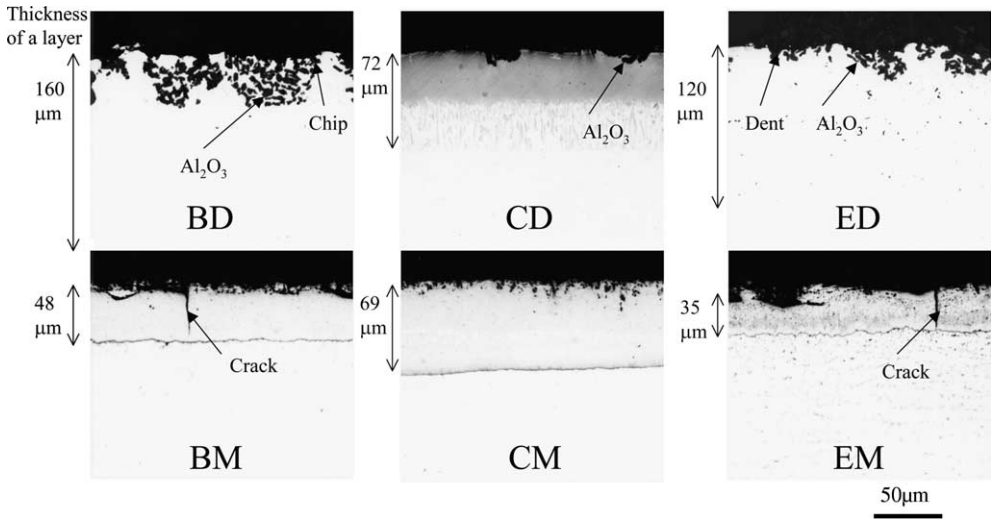

Fig. 1. Optical micrographs of cross-sections of Al-surface-treated steels. The thickness of layers produced by surface treatment is shown by arrows. The layers of BD, CD and ED contain Al_2O_3, $FeAl_2$ and $AlCr_2$. The layers of BM, CM and EM contain Fe_4Al_{13}, Fe_2Al_5, FeAl and Fe_3Al.

Table 3
X-ray diffraction results of some surface-treated steels before and after corrosion at 550 °C

	Al_2O_3	Fe_4Al_{13}	Fe_2Al_5	$FeAl_2$	FeAl	Fe_3Al	$AlCr_2$	$FeCr_2O_4$
BD								
As received	○			○			○	
After corrosion	○			○			○	
CD								
As received	○						○	
After corrosion	○						○	
ED								
As received	○			○			○	
After corrosion	○			○			○	△
BM								
As received			○		○	△		
after corrosion	△				○			
CM								
As received		○			○	△		
After corrosion	○				○			
EM								
As received		○	○		○	△		
After corrosion					○			

○: Large or medium intensity peak, △: small intensity peak.

micrographs. The thicknesses of the layers of AD, BD, CD, DD, ED and FD were 132, 160, 72, 150, 120 and 140 μm, respectively.

As shown in Fig. 1, surface-treated layers produced by the melt dipping method were also not uniform and contained cracks. Various types of Al compounds such as Fe_4Al_{13}, Fe_2Al_5, FeAl, Fe_3Al were formed as shown in Table 3. The thicknesses of the layers of AM, BM, CM, DM, EM and FM were 38, 48, 69, 41, 35 and 59 μm, respectively.

Corrosion specimens were rectangular plates with the size of 15 mm × 30 mm × 2 mm, and with a hole of 7.2 mm diameter at the top part of the specimen for installation.

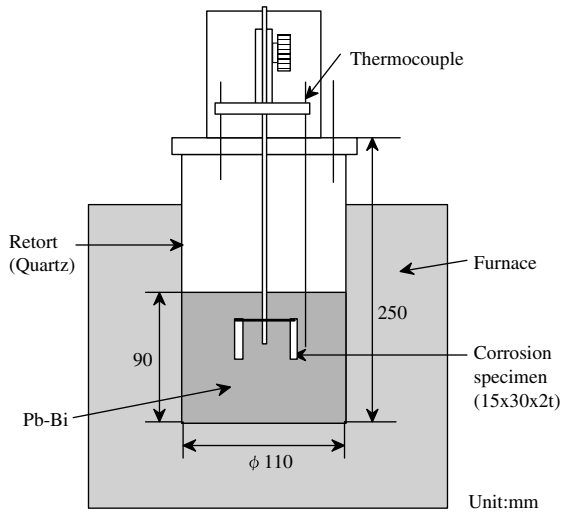

Fig. 2. Schematic of corrosion test apparatus in liquid Pb–Bi.

2.2. Corrosion test apparatus and test conditions

The corrosion test apparatus [9] is shown in Fig. 2. The retort was made of quartz which did not react with liquid Pb–Bi. As received eutectic Pb–Bi(45Pb–55Bi) of 7 kg was used in a test. Ar gas containing several percent of O_2 was used as stagnant cover gas over liquid Pb–Bi in order to make oxygen-saturated Pb–Bi at the test temperature. Although Al-surface treatment is expected to be effective for corrosion resistance under low oxygen concentration, oxygen-saturated Pb–Bi was used as the first phase of the research in this study. PbO was formed on the surface of the liquid Pb–Bi during the corrosion tests. Oxygen saturation concentration was estimated to be 3.2×10^{-4} wt% at 450 °C and 1.2×10^{-3} wt% at 550 °C using the equation in the literature [2]. Aluminum concentration in Pb–Bi after the corrosion test at 550 °C was estimated to be about 0.5 wt% from energy dispersion X-ray (EDX) analysis. Concentrations of Ni, Cr and Fe in Pb–Bi after the corrosion test at 550 °C were measured by inductively coupled plasma atomic-emission spectrometry (ICP-AES). The concentrations of Ni, Cr and Fe were $<4 \times 10^{-4}$ wt%, $<4 \times 10^{-4}$ wt% and $<2 \times 10^{-4}$ wt%, respectively. They are less than saturated ones, 3.21 wt% for Ni, 1.62×10^{-3} wt% for Cr and 6.01×10^{-4} wt% for Fe, respectively [2]. Corrosion tests were performed at 450 °C and 550 °C for 3000 h.

2.3. Analyses of specimens

Test specimens were pulled out from the liquid Pb–Bi and cooled in the cover gas. Although tested specimens were cleaned in silicone oil at about 170 °C, adherent Pb–Bi could not be removed from the specimen surface completely. X-ray diffraction measurements were made to identify corrosion products formed on the specimen surface. Furthermore, analyses using optical microscope, SEM (scanning electron microscope) and EDX (energy dispersion X-ray) were made after plating copper on the specimen surface to protect the corrosion films.

3. Experimental results and discussion

Corrosion tests were conducted using steel specimens with two kinds of Al-surface treatments as shown in

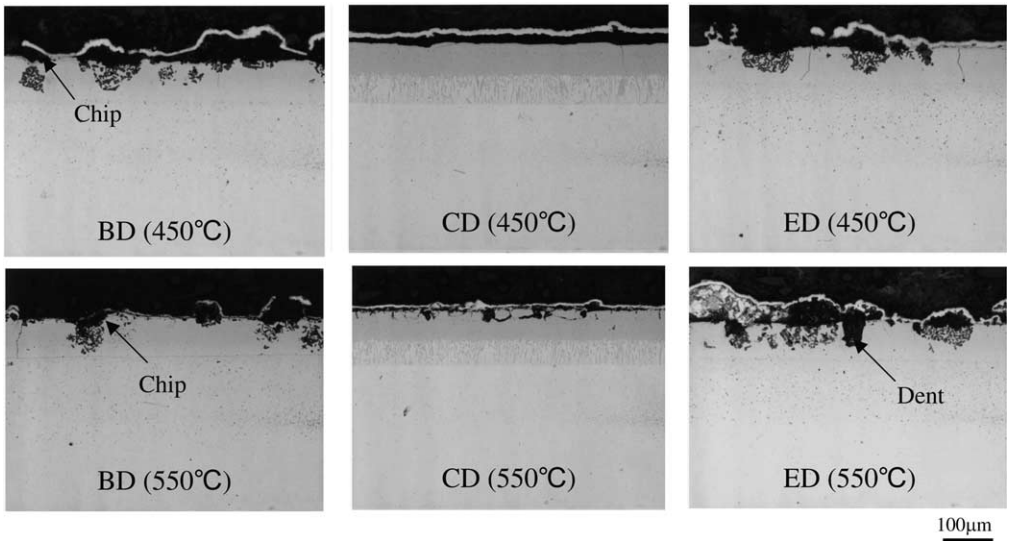

Fig. 3. Optical micrographs of cross-sections of Al-diffusion-treated specimens after corrosion test in liquid Pb–Bi at 450 °C and 550 °C for 3000 h.

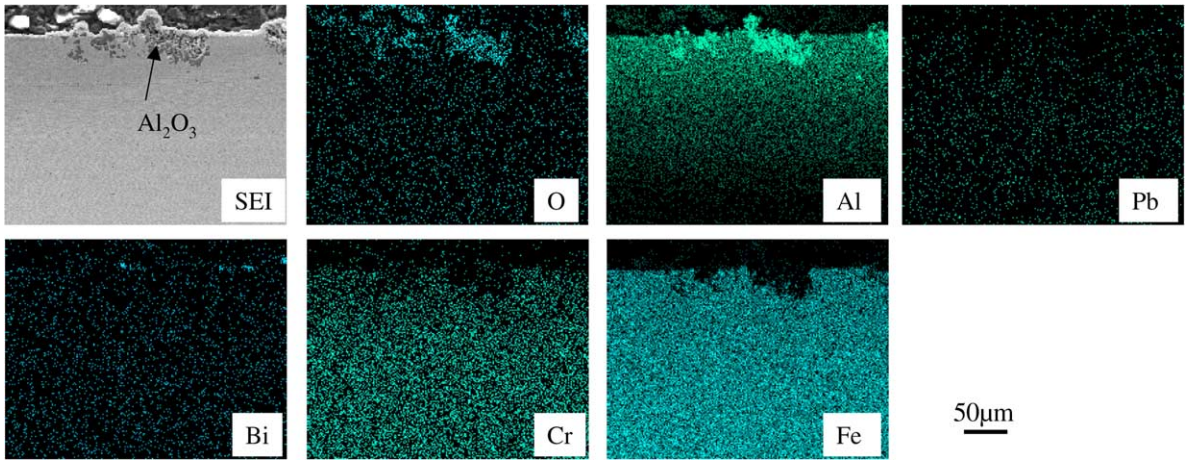

Fig. 4. EDX analysis of cross-sections of Al-diffusion-treated specimen (BD) after corrosion test in liquid Pb–Bi at 550 °C for 3000 h.

Table 2. Typical results of Al-surface-treated steels for steel B, C and E are described hereinafter.

Fig. 3 shows optical micrographs of the cross-sections of gas diffusion-treated specimens after the corrosion test. Dents and chips are observed on the surface layers of BD and ED. However, it was considered that the dents had already existed under as received condition as shown in Fig. 1. In the case of CD, the Al-surface-treated layer was sound at 450 °C as it was before the corrosion test. There was no corrosion damage on the surface-treated layer in all the specimens exposed to Pb–Bi at 550 °C except for fissures at the surface of the film. As shown in Table 3, the Al-surface-treated layer was composed of Al_2O_3, $FeAl_2$ and $AlCr_2$ in BD and ED, and Al_2O_3 and $AlCr_2$ in CD. Since X-ray diffraction peaks of these Al compounds remained after corrosion, it is considered that Al_2O_3, $FeAl_2$ and $AlCr_2$ formed on the surfaces of gas-diffusion-treated specimens were corrosion resistant to liquid Pb–Bi.

Fig. 4 shows the results of EDX analysis for the cross-section of BD specimen after corrosion at 550 °C for 3000 h. Concentration of Al was high near surface as shown in Fig. 4. Portions with high concentration of Al and O near surface contained Al_2O_3 according to Table 3. It is suggested in Fig. 1 that these large Al_2O_3 particles were formed at the stage of surface

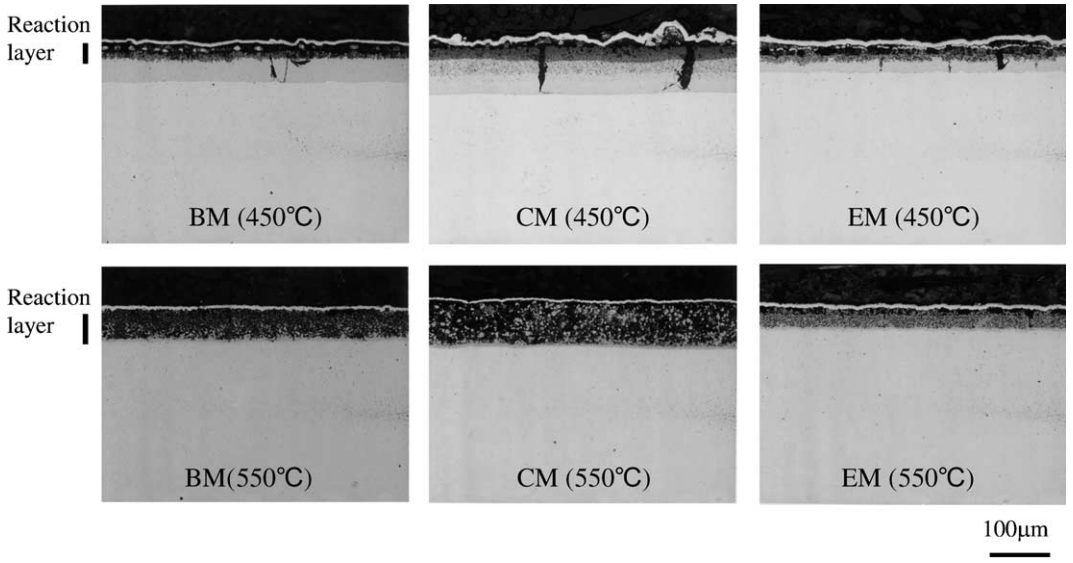

Fig. 5. Optical micrographs of cross-sections of Al melt dipping-treated specimens after corrosion test in liquid Pb–Bi at 450 °C and 550 °C for 3000 h.

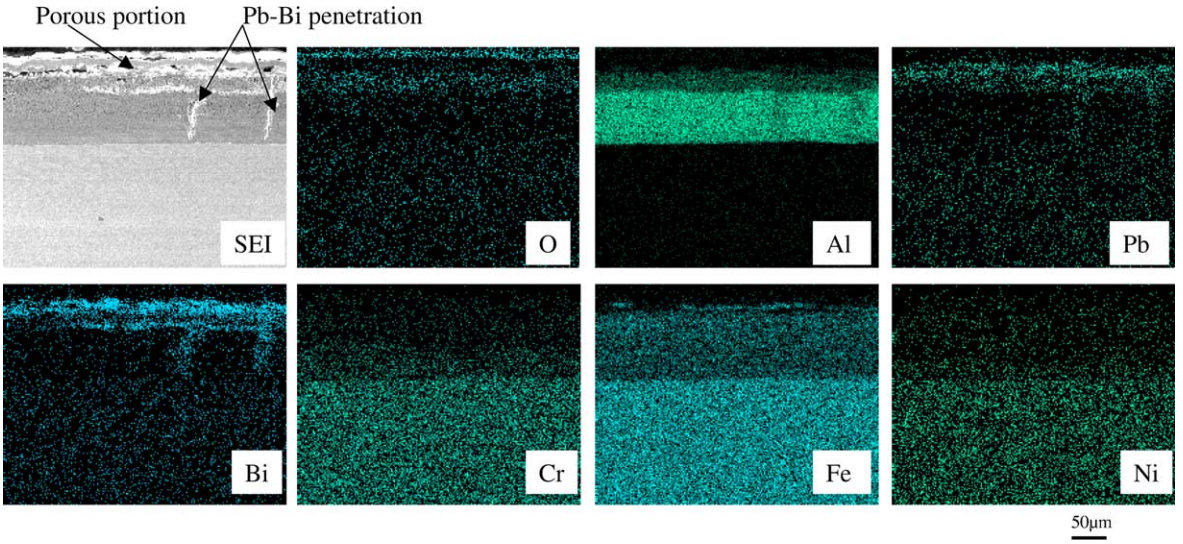

Fig. 6. EDX analysis of cross-sections of Al melt dipping-treated specimen (CM) after corrosion test in liquid Pb–Bi at 450 °C for 3000 h.

treatment. We can say that $FeAl_2$ and $AlCr_2$ existed from Table 3. There was no penetration of Pb and Bi into the surface-treated layer.

On the other hand, for specimens with melt dipping treatment as shown in Fig. 5, the reaction layer was observed at the surface region of the surface-treated layers in corrosion at 450 °C for 3000 h. All the surface-treated layers turned into the reaction layer in corrosion at 550 °C for 3000 h. A distinct corrosion attack to surface-treated layers was recognized. However, the corrosion attack by liquid Pb–Bi was restricted to the surface-treated layers. According to X-ray diffraction results of Table 3, Fe_4Al_{13} and Fe_2Al_5 that were identified before corrosion, disappeared during the corrosion test, and a small peak of Fe_3Al also seemed to disappear. Only FeAl was detected before and after corrosion test.

Fig. 6 shows the results of EDX analysis for the cross-section of CM specimen after corrosion at 450 °C

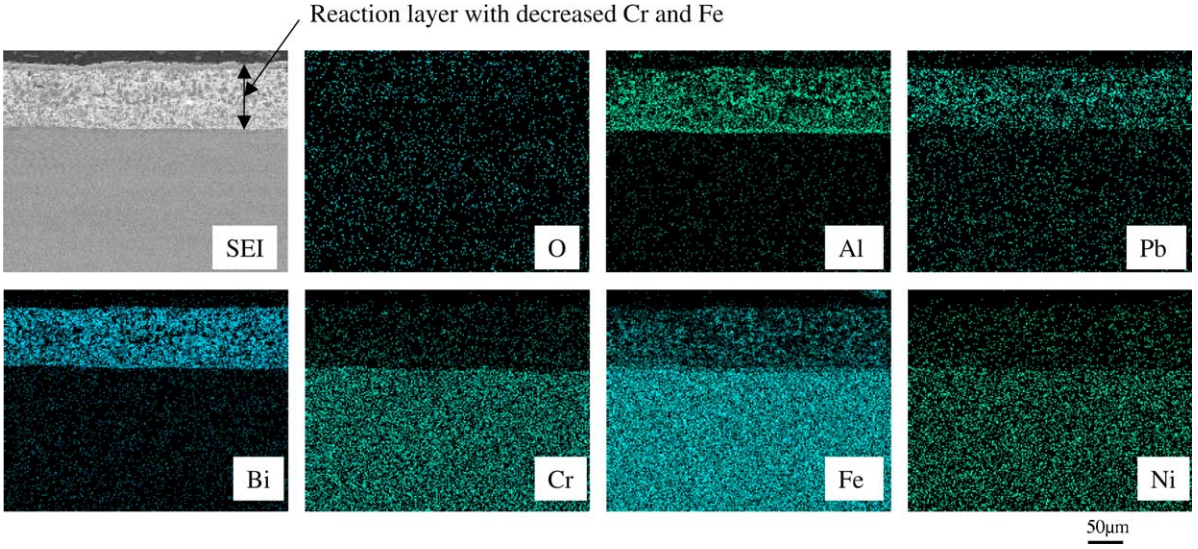

Fig. 7. EDX analysis of cross-sections of Al melt dipping-treated specimen (CM) after corrosion test in liquid Pb–Bi at 550 °C for 3000 h.

for 3000 h. Pb and Bi penetrated into porous regions of the reaction layer near surface where Al concentration decreased. Furthermore, they penetrated along the cracks of the surface-treated layer. As shown in Fig. 7, the results of EDX analysis for CM specimen after corrosion at 550 °C for 3000 h indicate that the surface-treated layer reacted with Pb and Bi, and only a few Al and Fe remained.

Mueller et al. reported that surface alloyed specimens containing FeAl had good corrosion resistance because of decrease in solution rate of Al and the formation of the stable oxide layer [12]. According to Hansen's phase diagram of Fe–Al binary alloy [15], Fe_3Al, FeAl, $FeAl_2$, Fe_2Al_5 and $FeAl_3$ existed as inter-metallic compounds. Fe_4Al_{13} observed in X-ray diffraction of this experiment would be a compound similar to $FeAl_3$. Since not only FeAl but also $FeAl_2$ and $AlCr_2$ remained after the corrosion test, these compounds would have corrosion resistance to liquid Pb–Bi. On the other hand, it was found that Al compounds of Fe_4Al_{13} and Fe_2Al_5 dissolved during the corrosion test. Corrosion resistance would basically decrease drastically in case of the existence of Fe_4Al_{13} and Fe_2Al_5 with high ratio of Al to Fe on account of the high solubility of Al in liquid Pb–Bi. Although the X-ray peak was weak, Fe_3Al also seemed to disappear during corrosion in liquid Pb–Bi in this experiment. Formation of uniform Al_2O_3 film on surface by pre-oxidation would be effective for improvement of corrosion resistance.

4. Conclusions

Corrosion tests of Al-surface-treated steels produced by gas diffusion and by melt dipping methods were conducted at 450 °C and 550 °C in a pot for 3000 h. The following conclusions are drawn:

(1) Al_2O_3, $FeAl_2$ and $AlCr_2$ were produced in the surface layer by the gas diffusion method. The surface-treated steels containing these compounds exhibited corrosion resistance to liquid Pb–Bi.

(2) Al-surface-treated layers by the melt dipping method reacted with Pb–Bi, and dissolution of Al and penetration of Pb and Bi occurred. Fe_4Al_{13} and Fe_2Al_5 produced by the melt dipping method disappeared during the corrosion test at 550 °C and only FeAl remained.

References

[1] T. Mukaiyama, T. Takizuka, M. Mizumoto, Y. Ikeda, T. Ogawa, A. Hasegawa, H. Takada, H. Takano, Prog. Nucl. Energy 38 (2001) 107.
[2] B.F. Gromov, Y.I. Orlov, P.N. Martynov, V.A. Gulevsky, Proceedings of Heavy Liquid Metal Coolants in Nuclear Technology, HLMC'98, 5–9 October 1998, Obninsk, Russia, 1999, p. 87.
[3] J.R. Weeks, Nucl. Eng. Design 15 (1971) 363.
[4] C. Rubbia, J.A. Rubio, S. Buono, F. Carminati, Conceptual design of a fast neutron operated high power energy amplifier, CERN/AT/95-44(ET), September 29, 1995.
[5] I.V. Gorynin, G.P. Karzov, V.G. Markov, V.S. Lavrukihin, V.A. Yakovlev, Proceedings of Heavy Liquid Metal Coolants in Nuclear Technology, HLMC'98, 5–9 October 1998, Obninsk, Russia, 1999 p. 120.
[6] F. Barbier, A. Rusanov, J. Nucl. Mater. 296 (2001) 231.
[7] Ph. Deloffre, A. Terlain, F. Barbier, J. Nucl. Mater. 301 (2002) 35.
[8] G. Benamti, C. Fazio, H. Piankova, A. Rusanov, J. Nucl. Mater. 301 (2002) 23.
[9] Y. Kurata, M. Futakawa, K. Kikuchi, S. Saito, T. Osugi, J. Nucl. Mater. 301 (2002) 28.
[10] G. Mueller, G. Schumacher, F. Zimmermann, J. Nucl. Mater. 278 (2000) 85.
[11] G. Benamati, P. Buttol, V. Imbeni, C. Martini, G. Palombarini, J. Nucl. Mater. 279 (2000) 308.
[12] G. Mueller, A. Heinzel, J. Konys, G. Schumacher, A. Weisenburger, F. Zimmermann, V. Engeliko, A. Rusanov, V. Markov, J. Nucl. Mater. 301 (2002) 40.
[13] R.C. Asher, D. Davies, S.A. Beetham, Corros. Sci. 17 (1977) 5445.
[14] H.U. Borgstedt, H. Glasbrenner, Fusion Eng. Des. 27 (1995) 659.
[15] M. Hansen, K. Anderko, Constitution of Binary Alloys, 2nd Ed., McGraw-Hill Book Company, 1989.